HHS Public Access

Author manuscript

J Inherit Metab Dis. Author manuscript; available in PMC 2020 September 01.

Published in final edited form as:

J Inherit Metab Dis. 2019 September ; 42(5): 944–954. doi:10.1002/jimd.12106.

Cln3-mutations underlying juvenile NCL cause significantly reduced levels of Ppt1-protein and Ppt1-enzyme activity in the lysosome

Abhilash P. Appu[*], **Maria B. Bagh**, **Tamal Sadhukhan**, **Avisek Mondal**, **Sydney Casey**, **Anil B. Mukherjee**[*]

Section on Developmental Genetics, Program on Endocrinology and Molecular Genetics, *Eunice Kennedy-Shriver* National Institute of Child Health and Human Development, National Institutes of Health, Bethesda, Maryland 20892-1830

Abstract

Mutations in at least 13 different genes (called *CLN*s) underlie various forms of neuronal ceroid lipofuscinoses (NCLs), a group of the most common neurodegenerative lysosomal storage diseases. While inactivating mutations in the *CLN1* gene, encoding palmitoyl-protein thioesterases-1 (PPT1), cause infantile NCL (INCL), those in the *CLN3* gene, encoding a protein of unknown function, underlie juvenile NCL (JNCL). PPT1 depalmitoylates S-palmitoylated proteins (constituents of ceroid) required for their degradation by lysosomal hydrolases and PPT1-deficiency causes lysosomal accumulation of autofluorescent ceroid leading to INCL. Since intracellular accumulation of ceroid is a characteristic of all NCLs, a common pathogenic link for these diseases has been suggested. It has been reported that *CLN3*-mutations suppress the exit of cation-independent mannose 6-phosphate receptor (CI-M6PR) from the trans Golgi network (TGN). Since CI-M6PR transports soluble proteins like PPT1 from the TGN to the lysosome, we hypothesized that *CLN3*-mutations may cause lysosomal PPT1-insufficiency contributing to JNCL pathogenesis. Here we report that the lysosomes in *Cln3*-mutant mice, which mimic JNCL, and those in cultured cells from JNCL patients, contain significantly reduced levels of Ppt1-protein and Ppt1-enzyme activity and progressively accumulate autofluorescent ceroid. Furthermore, in JNCL fibroblasts the V0a1 subunit of v-ATPase, which regulates lysosomal acidification, is mislocalized to the plasma membrane instead of its normal location on lysosomal membrane. This

[*]Correspondence to: A.P.A. (abhilash.appu@nih.gov) or ABM (mukherja@exchange.nih.gov).

AUTHOR CONTRIBUTIONS

A.B.M. conceived the project. A.P.P. and M. B.B. initiated the project; A.B.M. and M.B.B. supervised research; A. B.M., A.P.P. and M.B.B. designed the experiments; A.P.P., M.B.B., A.M., T.S. and S.C. performed most of the experiments; A.P.P., T.S and A.M. performed cell culture and culture-based experiments; A.P.P, M.B.B and A.M. performed confocal microscopy; A.P.P. performed Golgi and lysosome staining and colocalization experiments by confocal microscopy; A.P.P. and S. C. isolated lysosomes; A.P.P., and T.S. genotyped the mice; A.P.P. performed PPT1 enzymatic assays. A.B.M. wrote the first draft of the manuscript in which A.P.P. wrote the Methods section; The manuscript was edited by A.B.M with inputs from A.P.P., M.B.B, T.S., A.M. and S. C.

CONFLICT OF INTEREST

Abhilash P. Appu, Maria B. Bagh, Tamal Sadhukhan, Avisek Mondal, Sydney Casey and Anil B. Mukherjee declare that they have no conflict of interest.

INFORMED CONSENT

This article does not contain any studies with human subjects.

ANIMAL RIGHTS

All institutional and national guidelines for the care and use of laboratory animals were followed.

defect dysregulates lysosomal acidification, as we previously reported in *Cln1*$^{-/-}$ mice, which mimic INCL. Our findings uncover a previously unrecognized role of CLN3 in lysosomal homeostasis and suggest that *CLN3*-mutations causing lysosomal Ppt1-insuffiiciency may at least in part contribute to JNCL pathogenesis.

One sentence Summary:

CLN3 gene mutations cause drastic reduction in lysosomal PPT1-protein and PPT1-enzyme activity in a mouse model of JNCL.

Introduction

Neurodegeneration is a devastating manifestation in most lysosomal storage disorders (LSDs) (Proia and Wu 2004). Neuronal ceroid lipofuscinoses (NCLs) constitute a group of the most common neurodegenerative LSDs, which mostly affect children (Anderson et al 2013; Mole and Cotman 2015; Cárcel-Trullols et al 2015). Although for a few LSDs, treatments such as disease modifying therapy for Niemann Pick C disease (Patterson et al., 2007) and symptomatic treatments for epileptic seizures in the NCLs (reviewed in Mole et al. 2019) are currently available, there is no curative treatment for any of the neurodegenerative LSDs including the NCLs. While mutations in 13 distinctly different genes (called *CLN*s) underlie various forms of NCLs (Mole and Cotman, 2015), several clinical and pathological features are shared by all NCLs. For example, clinically all NCLs manifest early onset myoclonus and seizures, progressive loss of vision due to retinal degeneration, cerebral atrophy and shortened lifespan (Anderson et al 2013; Mole and Cotman 2015; Cárcel-Trullols et al 2015). At the cellular level, all NCLs show intracellular accumulation of autofluorescent ceroid. These common clinical and pathological features may suggest shared pathogenic links among various forms of NCLs. While inactivating mutations in the *CLN1* gene (Vesa et al 1995), encoding PPT1 (Camp et al 1994), cause infantile NCL (INCL) (Santavuori et al 1973), mutations in the *CLN3* gene, encoding a protein of unknown function, underlie juvenile NCL (JNCL) (International Batten Disease Consortium 1995).

Numerous proteins require post-translational lipid-modifications for their function. S-palmitoylation (also known as S-acylation) has emerged as the only reversible post-translational lipid-modification in which a 16-carbon saturated fatty acid (predominantly palmitate) is attached to specific cysteine residue(s) in polypeptides via thioester linkage (Fukata and Fukata 2010). While S-acylation plays important roles in regulating the stability and function of many proteins, especially in the brain (Huang and El-Husseini 2005), these lipid-modified proteins must also undergo depalmitoylation by thioesterases (e.g. PPT1) required for their degradation by lysosomal acid hydrolases (Lu et al 1996). The removal of palmitate from S-palmitoylated proteins catalyzed by PPT1 is essential for their recycling or degradation by lysosomal hydrolases (Camp and Hofmann 1993). Thus, it has been suggested that PPT1-deficiency leads to lysosomal accumulation of S-acylated proteins (constituents of autofluorescent ceroid) leading to INCL pathogenesis (Lu et al 1996), although the precise molecular mechanism of INCL remains unclear.

Mutations in the *CLN3* gene, which cause JNCL, encodes a 438-amino acid membrane-spanning protein of unknown function (Mole and Cotman 2015; Cárcel-Trullols et al 2015). It has been reported that one of the functions of the *CLN3* gene-product is to regulate the anterograde and retrograde post-Golgi trafficking (Cotman and Staropoli 2012). Most notably, it has been reported that *CLN3*-mutations suppress the exit of CI-M6PR from the TGN (Metcalf et al 2008). The CI-M6PR mediates the transport of soluble proteins (enzymes) like PPT1 from the TGN to the late endosome/lysosome (Braulke and Bonifacino 2009). In the present study, we tested a hypothesis that *CLN3* mutations, by suppressing the exit of CI-M6PR from the TGN, impair the transport and delivery of PPT1 to the lysosome and cause PPT1-insufficiency, thereby causing ceroid accumulation characteristically found in all NCLs including INCL and JNCL. Our results uncovered a previously unrecognized role of CLN3 in maintaining lysosomal homeostasis and suggest that there are shared pathological hallmarks between INCL and JNCL. These include disruption of trafficking of soluble proteins/enzymes from the TGN to the lysosome, leading to lysosomal PPT1-insufficiency, accumulation of autofluorescent ceroid and dysregulation of lysosomal pH.

Materials and Methods

Animals and treatments.

Wild type (WT) mice (C57BL/6J; Stock No. 000664) and *Cln3*-mutant mice (B6.129 (Cg)-*Cln3*$^{tm1.1Mem}$/J; Stock No.017895) with homogeneous C57BL/6J background were purchased from the Jackson Laboratory (Bar Harbor, ME). All animals were housed in a pathogen-free facility with 12 h light/12 h dark cycles with access to water and food ad libitum. All the mice were genotyped according to the protocol of Jackson Laboratory. The animal procedures were carried out according to an animal study protocol (#16–012) approved by the *Eunice Kennedy Shriver* National Institute of Child Health and Human Development (NICHD), NIH, Animal Care and Use Committee (ACUC).

Chemicals

Phosphate Buffered Saline (PBS) (Cat # 10010023) and LysoSensor Green DND 189 (Cat # L7535) were purchased from ThermoFisher Scientific, Rockford, IL. β-Mercaptoethanol (Cat #M6250), Na_2CO_3 and $NaHCO_3$ were from Sigma Aldrich, St. Louis, MO. Paraformaldehyde (Cat #15710) was purchased from Electron Microscopy Sciences, Hatfield, PA.

Cells and Cell culture

The normal human fibroblasts (GM00498) were obtained from Coriell Institute for Medical Research. CLN3 patient fibroblasts (C8614 and C9282) were obtained from the laboratory of late Dr. K. E. Wisniewski, New York State Institute for Basic Research. These patient cells have identical mutations (i.e. homozygous 1.02kb deletion in the *CLN3* gene) as previously reported (Wang et al. 2011; Zhong, 2001). Normal and CLN3 patient fibroblasts were cultured in DMEM (ThermoFisher scientific; Cat # 11965–092) with 10% fetal bovine serum (FBS) and 1% Penstrep (ThermoFisher scientific; Cat # 15140–122). Cells were maintained at 37°C in a humidified 5% CO_2 atmosphere. Before all experiments, we

replaced DMEM with Opti-MEM (ThermoFisher scientific; Cat #31985–070) and cultured the cells overnight without fetal bovine serum (FBS) as it contains Ppt1-activity.

Purification of the lysosomal fractions.

Lysosomal fractions were isolated from mouse brain cortex using Optiprep density gradient media using the lysosome isolation kit (Sigma-Aldrich; Cat #LYSISO1) as per manufacturer's protocol. The enrichment of lysosomes in the lysosomal fractions was assessed by Western blot analysis using antibody to a lysosomal membrane marker, LAMP II. Fractions 2 and 3 were found to be lysosome-enriched and were combined for all assays and immunoblotting experiments.

PPT1-enzyme activity assay

Enzymatic activity of Ppt1 was measured as previously reported (Van Diggelen et al 1999). Briefly, total homogenate and lysosomal fractions were further diluted in PBS and sonicated. The samples (10 μg protein) were incubated with the substrate 4-Methylumbelliferyl-6-thiopalmitoyl-b-D-glucoside (Moscerdam Substrates, the Netherlands) for 1 h at 37°C as described in the manufacturer's protocol. The reaction was terminated by the addition of Stop Buffer (0.5M Na_2CO_3/$NaHCO_3$, pH 10.7, 0.025% Triton X-100). The fluorescence of the product, 4- Methylumbelliferone, was measured FlexStation II spectrofluorometer (Molecular Devices, Sunnyvale, CA) at absorbance wavelengths of 355 nm, λ_{ex} and 460 nm, λ_{em}. Activities were calculated according to the instructions provided by the substrate manufacturer (Moscerdam Substrates).

Confocal imaging

Fibroblasts from CLN3 patients and age- and sex matched normal control subjects were cultured in 8 well chamber slides with DMEM washed 2 to 3 times with PBS and cells were fixed using 100% methanol. Then the cells were washed with PBS and blocked with 10% normal goat serum for 1 h., the cells were incubated with primary antibodies overnight at 4°C for 1 h at room temperature. The primary antibodies used were: Ppt1 (a gift from Dr. S.L. Hofmann; Dilution 1:1000), CIM6PR (Abcam, Cat #ab124767; Dilution 1:1000), LAMP2 (EMD Millipore; Cat #MABC40; Dilution 1:200) GM-130 (BD Biosciences, Cat #610823; Dilution 1:1,500), V0a1 (Abnova; Cat #H00000535-A01; Dilution 1:100), Na^+ K^+ ATPase (Cell Signaling, Cat#3010S; dilution 1:200) followed by Alexa Fluor-conjugated secondary antibodies (Invitrogen). Cells were mounted using DAPI-Fluoromount G (Thermo Fisher, 010020) and fluorescence was visualized with the Zeiss LSM 710 Inverted Meta confocal microscope (Carl Zeiss). Each experiment was repeated at least 3 times with 10 cells analysed per experiment per group (Total 30 cells per group). The image was processed with the LSM Image Software (Carl Zeiss 710) and Pearson's colocalization coefficient (Dunn et al. 2011) was calculated (Dunn et al. 2011) using the Zen Desk Software from Zeiss.

Western blot analysis.

For Western blot, protein samples (20 μg) were resolved by electrophoresis using 4–12% SDS–polyacrylamide gels (Invitrogen) under denaturing and reducing conditions and blotted

to nitrocellulose or polyvinylidene difluoride membranes (Invitrogen). The membranes were blocked with 5% nonfat dry milk (Bio-Rad) and then subjected to immunoblot analysis using standard methods. The primary antibodies used for the immunoblots were as follows: Ppt1 (Hofmann Lab; dilution 1:1000) and LAMP2 (EMD Millipore, Cat#MABC40; dilution 1:1000). The blots were then probed with HRP-conjugated secondary antibodies (Santa Cruz Biotechnology) followed by detection using SuperSignal west femto or pico solution (Thermo Fisher Scientific) according to the manufacturer's instructions. Image quant 4000 mini (GE Healthcare Lifesciences) was used to capture the chemiluminescent signals, and the immunoblots were quantitated using the image quant TL software (GE Healthcare Lifesciences). Experiments were repeated at least four times to confirm the reproducibility.

Autofluorescence

The method for detecting autofluorescence has been described previously (Zhang et al 2006) Briefly, the tissues were fixed in 4.0% paraformaldehyde, embedded in paraffin, and processed for histological sectioning (Histoserv Inc, Germantown, MD). The slides with the tissue sections were dipped in xylene for 5 min to remove paraffin and then successively passed through decreasing concentrations of ethanol (100–0%) in water. The sections were then mounted with Vectashield Mounting Medium (Vector Laboratories, Burlingame, CA, Lot #R0712) and covered with cover slips. Autofluorescence was visualized using the EVOS FL Auto microscope under green fluorescent light.

Determination of total lysosomal palmitoylated proteins by Acyl-RAC Assay

To determine the lysosomal-total palmitoylated proteins, we performed Acyl-RAC assay as previously reported by Forrester et al. (Forrester et al 2011). Lysosomal fractions (250μl each) containing 1 mg protein were used for this assay. The S-palmitoylated (bound) and non-S-palmitoylated (unbound) proteins were further processed for Western blot. Both S-palmitoylated and non-S-palmitoylated protein fractions were resolved by SDS-PAGE. The gels were silver stained as per manufacture's protocol (Pierce Silver Stain Kit, Thermo scientific, Cat No- 24612). Images were acquired by Image Quant LAS4000 imager and quantitated using the Image Quant TL software (GE Healthcare Lifesciences).

Determination of lysosomal pH

To check lysosomal pH qualitatively, both normal and patient fibroblasts were cultured in DMEM for two days, followed by Opti-MEM for one. Then the fibroblasts were labelled with 1 mM pH-sensitive lysosensor green DND-189 (L-7535, Life Technologies-Thermo Fisher Scientific) for 10 min at 37°C, washed with PBS (two to three times), then imaged using a fluorescein isothiocyanate channel in FluoroBrite DMEM media. To measure the lysosomal pH, we used Oregon green dextran (Life Technologies, D-7172) and TMR dextran (D-1819; Life Technologies (Thermo Fisher Scientific), as previously reported (Haggie and Verkman 2009) with minor modifications (Bagh et al., 2017; Perera et al 2015; Zoncu et al 2011). Briefly, the lysosomal pH was measured by using the fluorescence ratio between the pH-sensitive Oregon green (ex-496, em-524) and pH insensitive TMR (ex-555, em-580). For the confirmation of co-localization of Oregon green and TMR dextran, both normal and patient fibroblasts were grown on chamber slide. The cells were then incubated with Oregon green-dextran (1mg/ml) and TMR dextran (1 mg/ml) in the media for 1 h.

washed and chased with Opti-MEM for 4 hrs. for dextran to accumulate in lysosomal compartment. Hoechst stain used as a nuclear marker. Then the image was captured with the Zeiss LSM 710 Inverted Meta confocal microscope (Carl Zeiss). It showed 100% colocalization of Oregon green and TMR dextran in both normal and patient fibroblasts (Fig. S3D).

For the quantitative measurement, both normal and patient fibroblasts were cultured in DMEM for a week and replaced with Opti-MEM for one day, then incubated with Oregon green-dextran (1mg/ml) and TMR dextran (1 mg/ml) in the media for 1 h. and washed with Opti-MEM and further incubated in the Opti-MEM for 4 h for dextran to accumulate in late endosomal/lysosomal compartment. Then the cells were harvested by cell scraper, counted and washed four times in PBS and resuspended in MES calibration buffer solution of varying pH containing 5 mM NaCl, 115 mM KCl, 1.2 mM MgSO4 and 25 mM MES in the presence of 10 mM nigericin and 10 mM monencin. Equal number of cells were transferred to black 96 well microplate and the fluorescence intensity was measured by Flex Station- II (Molecular Devices, CA). Then a standard curve was plotted by using the intensities of green fluorescence versus red fluorescence emission against standard pH and determined the unknown pH by extrapolating the standard curve (S3C). Both normal and patient fibroblasts were loaded with the pH sensors and resuspended in the same calibration buffer without nigericin and monencin for measuring the pH.

Statistical analysis

The results were analyzed using GraphPad Prism-7. One-way ANOVA was used for comparison among the groups; $p \leq 0.05$ was considered significant. All the experiments were repeated at least three times.

Results

Reduced levels of lysosomal Ppt1-protein and Ppt1-enzymatic activity in *Cln3*-mutant mice

The mutations in the *CLN3* gene, which underlie JNCL, prevent the exit of CI-M6PR from the TGN (Metcalf et al 2008). The CI-M6PR transports soluble proteins like PPT1 from the TGN to the late endosomal/lysosomal compartment (Fig. 1A). We speculated that in *Cln3*-mutant mice, which mimic JNCL, and cultured cells from JNCL patients defective exit of CI-M6PR from the TGN may impair the delivery of Ppt1 to the lysosome (Fig. 1B). This may lead to Ppt1-insufficiency and contribute to progressive accumulation of ceroid in the lysosome. To address this question, we first determined the levels of CI-M6PR colocalization with the Golgi marker, GM-130. by confocal microscopy and Pearson's colocalization coefficient analysis. The results showed that CI-M6PR and GM-130 colocalization was significantly higher in JNCL patient fibroblasts compared with that in normal fibroblasts (Fig. 2A). These results confirmed the previous report that *CLN3*-mutations suppress the exit of CI-M6PR from the TGN (Metcalf et al 2008). We then sought to determine whether the delivery of Ppt1-protein to the lysosome was reduced in JNCL patient fibroblasts. Accordingly, we performed confocal microscopy to determine the level of colocalization of PPT1-immunofluorescence with that of the lysosomal marker, LAMP2. We found that while in normal fibroblasts there was a high level of colocalization of PPT1

fluorescence with that of LAMP2-fluorescence (Fig. 2B, upper panels), in the JNCL fibroblasts such colocalization was substantially lower (Fig. 2B, lower panels). We then measured the levels of Ppt1-protein in the lysosomal fractions of brain tissues from WT and *Cln3*-mutant mice by Western blot analysis. The results showed that the Ppt1-protein levels in the lysosome from the brain of *Cln3*-mutant mice were significantly lower compared with those of the WT mice (Fig. 2C). We then determined the Ppt1-enzymatic activities in lysosomal fractions from brain tissues of WT and *Cln3*-mutant mice. The results showed that the Ppt1-enzymatic activities in the lysosomal fractions from the brain of *Cln3*-mutant mice were also significantly lower compared with those of the WT controls (Fig. 2D). Moreover, we determined the lysosomal PPT1-activity in cultured cells from a JNCL patient and those from an age- and sex-matched normal control subject. The results showed that the JNCL patient's cells had a markedly lower PPT1-enzymatic activity compared with that of the normal control (Fig. 2E). Since the Ppt1-protein levels were lower in the lysosomes from *Cln3*-mutant mouse brain, we determined the Ppt1-mRNA levels by qRT-PCR using total RNA from the brains of WT and *Cln3*-mutant mice. The results showed that there was no significant difference in the Ppt1-mRNA levels between WT and *Cln3*-mutant mice (Supplementary Fig. S1A). Taken together, these results suggested that *Cln3* mutations impair CI-M6PR exit from the TGN causing increased levels of CI-M6PR in the TGN and consequently, reduced levels of Ppt1 in the lysosome causing lysosomal Ppt1-insufficiency in these mice.

Increased autofluorescence and S-acylated protein levels in the brain of *Cln3*-mutant mice

It has been reported that lysosomal Ppt1-deficiency prevents the degradation of S-palmitoylated proteins causing intracellular ceroid accumulation leading to INCL (Lu et al 1996). We sought to determine whether intracellular autofluorescence progressively increased with age in the brain tissues of *Cln3*-mutant mice. Consistent with the reduced levels of Ppt1-protein and Ppt1-enzymatic activity in the lysosome, our results showed that compared with WT mice, the levels of autofluorescence in the brain of *Cln3*-mutant mice progressively increased with age (Fig. 3A). Next, we determined the levels of total S-palmitoylated proteins in the brain tissues from WT and *Cln3*-mutant mice by acyl-RAC assay (Forrester et al 2011). The results showed that there were progressively increased levels of total S-palmitoylated protein accumulation in the brain of *Cln3*-mutant mice in an age-dependent manner (Fig. 3B). Taken together, these results demonstrated that *Cln3*-mutations cause lysosomal Ppt1-insufficiency, which most likely leads to progressive intracellular accumulation of autofluorescent material (ceroid).

Dysregulation of lysosomal acidification in cultured JNCL fibroblasts

In virtually all LSDs, dysregulation of lysosomal acidification impairs the activity of various acid hydrolases, which suppresses their degradative capability causing lysosomal accumulation of undegraded cargo. Lysosomal acidification is regulated by v-ATPase (Forgac 2007), a multi-subunit protein localized to the lysosomal membrane. Previously, we reported that in *Cln1*$^{-/-}$ mice (Gupta et al 2001), which mimic INCL (Bible et al 2004) and in cultured fibroblasts from INCL patients, PPT1-deficiency causes misrouting of a critical subunit of v-ATPase, V0a1, to the plasma membrane instead of its normal location to the lysosomal membrane dysregulating lysosomal acidification (Bagh et al 2017). Thus, we first

sought to determine whether lysosomal pH is dysregulated in cultured JNCL patient fibroblasts. Accordingly, we stained the cells with a fluorescent dye, DND-189 dextran. The fluorescence of the cells inversely correlates with lysosomal pH and is used to qualitatively assess the lysosomal pH in a cell. The results showed that compared to normal fibroblasts, DND-189 fluorescence in JNCL fibroblasts was substantially lower, which suggests an elevated lysosomal pH (Fig. 3C). Next, we performed a quantitative measurement of the lysosomal pH by double-labeling the normal and JNCL patient fibroblasts using a pH-sensitive fluorescent dye, Oregon green and a pH-insensitive dye, tetramethyl rhodamine (TMR) dextran. The ratiometric analyses of the two fluorescence intensities were performed. Also, we have confirmed the complete co-localization of Oregon green and TMR dextran by confocal microscopy (Fig. S3D). The results showed that lysosomal pH in cultured fibroblasts from JNCL patients is substantially higher compared with that of the normal fibroblasts (Fig. 3D).

Misrouting of V0a1 of v-ATPase to the plasma membrane in JNCL fibroblasts

We sought to determine the cause of increased lysosomal pH in JNCL fibroblasts. Previously, we reported that Ppt1-deficiency leads to the misrouting of the V0a1 subunit of the v-ATPase to the plasma membrane dysregulating lysosomal pH in cultured neurons from *Cln1*$^{-/-}$ mice (Bagh et al 2017). Thus, we sought to determine whether *Cln3*-mutations causing PPT1 insufficiency in cultured JNCL fibroblasts V0a1 is mislocalized to the plasma membrane and not to its normal location on lysosomal membrane. Accordingly, we performed confocal microscopic imaging to determine the colocalization of V0a1-immunofluorescence with that of the LAMP2 fluorescence (a lysosomal marker) in cultured normal and JNCL fibroblasts. The results clearly demonstrated that while V0a1 predominantly colocalized with the lysosomal membrane marker, LAMP2 in normal fibroblasts (Fig. 3E, **upper panels**), such colocalization was virtually undetectable in JNCL fibroblasts (Fig. 3E, **lower panels**). To determine whether V0a1 is misrouted to the plasma membrane of JNCL fibroblasts, which we previously reported in INCL fibroblasts (Bagh et al 2017), we performed confocal microscopy using antibodies to V0a1 and antibodies to a plasma membrane marker, Na^+ K^+-ATPase. Our results showed that while most of the V0a1-immunofluorescence in normal fibroblasts did not colocalize with that of the plasma membrane marker, Na^+K^+ ATPase (Fig. 3F, **upper panels**), that in the JNCL fibroblasts colocalized with the Na^+ K^+-ATPase (Fig. 3F, **lower panels**). Cumulatively, these results suggested that JNCL fibroblasts harboring *CLN3* mutations show many of the pathologic features of PPT1-deficient cells from INCL patients and suggest that lysosomal PPT1-insufficiency may be one of the contributing factors in JNCL pathogenesis.

Discussion

In this study, we demonstrate for the first time that in *Cln3*-mutant mice and in JNCL patient fibroblasts there is significantly reduced levels of lysosomal PPT1-protein and PPT1-enzymatic activity. We also demonstrate that consistent with a previous report (Metcalf et al 2008), the exit of CI-M6PR from the TGN is disrupted in *Cln3*-mutant mice. This defect most likely is the cause of substantially reduced levels of PPT1-protein and PPT1-enzymatic activity in the lysosome of *CLN3*-mutant cells. Notably, in the brain of *Cln3*-mutant mice

the Ppt1-mRNA (Supplementary Fig. S1A), Ppt1-protein (Supplementary Fig. S1B) as well as Ppt1-enzymatic activity (Supplementary Fig. S1C) were virtually identical to those in WT controls. These results suggest that *CLN3*-mutations disrupt the trafficking of PPT1 from the TGN to the lysosomal lumen in JNCL cells. Furthermore, we found increased levels of polyubiquitinated proteins (Supplementary Fig. S2A) and proteasome activity (Supplementary Fig. S2B) in the brain tissues of *Cln3*-mutant mice, which may suggest that autophagy is dysregulated as we have also observed in PPT1-deficient INCL fibroblasts. Taken together, these results suggested that proteins, including PPT1, may be degraded at a higher rate in both $Cln1^{-/-}$ and *Cln3*-mutant mice via ubiquitin-proteasome pathway.

To determine the specificity of PPT1-insufficiency in cells in which *CLN3* is mutated, we measured a lysosomal enzyme, β-glucocerebrosidase (β-GBA), the deficiency of which underlie Gaucher's disease (Stone et al 2000). Moreover, β-GBA is transported from the TGN to the lysosome by LIMP2 (Reczek et al 2007) and not by CI-M6PR. Our results showed that while there is lysosomal Ppt1-insufficiency in the brain tissues of *Cln3*-mutant mice as well as in cultured JNCL cells, the levels of β-GBA-protein (Supplementary Figs. S3A) and β-GBA-enzyme activity (Supplementary Figs. S2B) in lysosomal fractions were unaltered. These results suggested that *CLN3*-mutations selectively affect those proteins/enzymes like PPT1 that are transported by CI-M6PR, but not those like β-GBA, which are transported by a receptor other than CI-M6PR like LIMP2. Thus, our findings demonstrate that lysosomal Ppt1-insufficiency in *Cln3*-mutant mice and in cultured JNCL fibroblasts is a specific defect resulting from *CLN3*-mutations, which prevent the exit of CI-M6PR from the TGN (Metcalf et al 2008). Consistent with these findings, the natural histories of INCL and JNCL show that the former is an early onset (11–18 months of age), rapidly progressive disease while the latter is a relatively late onset (5–6 years of age) and slowly progressive disease. This may be because INCL is caused by inactivating mutations of the *CLN1*-gene causing a complete deficiency of PPT1-activity (Vesa et al 1995) and JNCL results from *CLN3*-mutations causing lysosomal PPT1-insifficiency due to the defective exit of CI-M6PR from the TGN (Metcalf et al 2008). Taken together, our results show that the accumulation of total S-palmitoylated proteins (ceroid) in the lysosome from $Cln3^{-/-}$ mouse brain occurs slowly, which is consistent with the slower onset of disease manifestation in these mice as well as in JNCL patients.

Altered lysosomal pH is an important pathological finding in several NCLs (Holopainen et al 2001) including INCL (Bagh et al 2017) and JNCL (Cárcel-Trullols et al 2015). Lysosomal acidification is regulated by v-ATPase, a multi-subunit protein complex with a membrane-anchored V0 sector and a cytosolic V1 sector (Forgac 2007). It is noteworthy that both V0a1 (Bagh et al 2017) as well as CI-M6PR (Schweizer et al 1996; McCormick et al 2008) require dynamic S-palmitoylation for their trafficking to the lysosomal membrane. We recently uncovered that V0a1, which undergoes dynamic S-palmitoylation, anchors to the lysosomal membrane upon which the other subunits (i.e. V1) assemble to generate the functional v-ATPase (Bagh et al 2017). Moreover, in Ppt1-deficient, $Cln1^{-/-}$ mice, V0a1 subunit is misrouted to the plasma membrane instead of its normal location on lysosomal membrane (Bagh et al 2017). Thus, it is likely that due to Ppt1-insufficiency in *Cln3*-mutant mice and in JNCL cells, V0a1 transport to the lysosomal membrane is altered impairing v-ATPase activity, thereby, elevating lysosomal pH. Since most lysosomal enzymes including

the acid hydrolases have an acidic pH optimum, their ability to degrade the undigested cargo delivered to the lysosome may impaired causing accumulation of ceroid, which contributes to JNCL pathogenesis.

It is estimated that inactivating mutations in one copy of a gene may lead to reduced level of protein and as a result it can cause human disease. This condition has been termed haploinsufficiency. Currently, it has been estimated that haploinsufficiency of more than 600 genes underlie various human diseases and recently, it has been reported that activation of a promoter or enhancer by CRISPR rescues obesity caused by haploinsufficiency (Matharu et al. 2019). While it is generally believed that in autosomal recessive diseases the heterozygotes are phenotypically normal, it is increasingly evident that haploinsufficiency of a gene product may lead to phenotypic manifestations that are different from that of the complete absence of the same gene product. For example, while the complete deficiency of β-GBA causes type-2 Gaucher's disease (Stone et al 2000), haploinsufficiency of β-GBA may manifest as Parkinson's disease in humans (Sidransky et al 2009) and in mice (Tayebi et al 2017). Moreover, it has been reported that while complete ablation of the *CLN11* gene encoding progranulin causes NCL11-disease in humans (Canafoglia et al 2014) and in mice (Hafler et al 2014), its haploinsufficiency manifests as frontotemporal dementia (Paushter et al 2018). While inactivating mutations in the *CLN1* gene encoding PPT1 cause INCL, the results of our present study demonstrate that nearly 50% of lysosomal PPT1-activity is found in *CLN3*-mutant cells raising the possibility that this defect at least in part contribute to JNCL pathogenesis. This is not to say that lysosomal PPT1-insufficiency causes JNCL phenotype, because obviously the function(s) of the CLN3-protein is yet to be uncovered although its deficiency leads to JNCL pathogenesis. It is possible that the heterozygotes in an autosomal recessive disease, like the LSDs, while phenotypically normal, may have subtle defects that may not manifest as overt disease phenotype. At this juncture, it is not entirely clear what parameter(s) one may look for to detect such subtle changes in the heterozygotes in autosomal recessive diseases, which demonstrate insufficiency of a gene product like PPT1.

Recently, mechanism-based development of small molecules that crosses the blood-brain-barrier have been proposed for the treatment of neurodegenerative diseases (Kinarivala and Trippier 2016). Moreover, we have reported the identification of a Ppt1-mimetic, small molecule, N-tert (Butyl) hydroxylamine (NtBuHA), that has neuroprotective and lifespan extending properties in *Cln1*$^{-/-}$ mice (Sarkar et al 2013). It would be of interest to determine whether brain-penetrant, Ppt1-mimetic small molecules such as NtBuHA may be beneficial for both INCL and JNCL. The validity of this hypothesis may be tested using *Cln3*-mutant mice.

Supplementary Material

Refer to Web version on PubMed Central for supplementary material.

ACKNOWLEDGEMENTS

We thank J.Y. Chou and S.W. Levin for critical review of the manuscript and helpful suggestions. We also thank Dr. V. Schram (Microscopy and Imaging Core, *Eunice Kennedy-Shriver* National Institute of Child Health and Human

Development [NICHD]) for his help with confocal microscopy. This research was supported in full by the Intramural Research Program of the *Eunice Kennedy Shriver* NICHD, NIH. The content is solely the responsibility of the authors and does not necessarily represent the official views of the National Institutes of Health.

References

Anderson GW, Goebel HH, Simonati A (2013) Human pathology in NCL. Biochim Biophys 1832: 1807–1826.

Bagh MB, Peng S, Chandra G et al. (2017) Misrouting of v-ATPase subunit V0a1 dysregulates lysosomal acidification in a neurodegenerative lysosomal storage model. Nat Commun 8: 14612. [PubMed: 28266544]

Bible E, Gupta P, Hofmann SL et al. (2004) Regional and cellular neuropathology in the palmitoyl protein thioesterase-1 null mutant mouse model of infantile neuronal ceroid lipofuscinosis Neurobiol Dis 16: 346–359. [PubMed: 15193291]

Braulke T, Bonifacino JS (2009) Sorting of lysosomal proteins. Biochim Biophys Acta 1793: 605–614. [PubMed: 19046998]

Camp LA, Hofmann SL (1993) Purification and properties of a palmitoyl-protein thioesterase that cleaves palmitate from H-Ras. J Biol Chem. 268:22566–22574. [PubMed: 7901201]

Camp LA, Verkruyse LA, Afendis SJ et al. (1994) Molecular cloning and expression of palmitoyl-protein thioesterase. J Biol Chem 269: 23212–23219. [PubMed: 7916016]

Canafoglia L, Morbin M, Scaioli V et al. (2014) Recurrent generalized seizures, visual loss, and palinopsia as phenotypic features of neuronal ceroid lipofuscinosis due to progranulin gene mutation. Epilepsia 55: 56–59.

Cárcel-Trullols J, Kovács AD, Pearce DA (2015) Cell biology of the NCL proteins: What they do and don't do. Biochim Biophys Acta 1852: 2242–2255. [PubMed: 25962910]

Cotman SL, Staropoli JF (2012) The juvenile Batten disease protein, CLN3, and its role in regulating anterograde and retrograde post-Golgi trafficking. Clin Lipidol 7: 79–91. [PubMed: 22545070]

Dunn KW, Kamocka MM, McDonald JF (2011) A practical guide to evaluating colocalization in biological microscopy. Am J Physiol Cell Physiol 300: C723–C742. [PubMed: 21209361]

Forgac M (2007) Vacuolar ATPases: rotary proton pumps in physiology and pathophysiology. Nat Rev Mol Cell Biol 8: 917–929. [PubMed: 17912264]

Forrester MT, Hess DT, Thompson JE et al. (2011) Site-specific analysis of protein S-acylation by resin-assisted capture. J Lipid Res 52: 393–398. [PubMed: 21044946]

Fukata Y, Fukata M (2010) Protein palmitoylation in neuronal development and synaptic plasticity. Nat Rev Neurosci 11: 161–175. [PubMed: 20168314]

Gupta P, Soyombo AA, Atashband A et al. (2001) Disruption of PPT1 or PPT2 causes neuronal ceroid lipofuscinosis in knockout mice. Proc Natl Acad Sci U S A 98: 13566–13571. [PubMed: 11717424]

Hafler BP, Klein ZA, Jimmy Zhou et al. (2014) Progressive retinal degeneration and accumulation of autofluorescent lipopigments in progranulin deficient mice. Brain Res 1588: 168–174. [PubMed: 25234724]

Haggie PM, Verkman AS (2009) Unimpaired lysosomal acidification in respiratory epithelial cells in cystic fibrosis. J Biol Chem 284: 7681–7686. [PubMed: 19136560]

Holopainen JM, Saarikoski J, Kinnunen PKJ et al. (2001) Elevated lysosomal pH in neuronal ceroid lipofuscinoses (NCLs). Eur J Biochem 268: 5851–5856. [PubMed: 11722572]

Huang K, El-Husseini A (2005) Modulation of neuronal protein trafficking and function by palmitoylation. Curr Opin Neurobiol 15: 527–535. [PubMed: 16125924]

International Batten Disease Consortium (1995) Isolation of a novel gene underlying Batten disease, CLN3. Cell 82: 949–957. [PubMed: 7553855]

Kinarivala N, Trippier PC (2016) Progress in the development of small molecule therapeutics for the treatment of neuronal ceroid lipofuscinoses (NCLs). J Med Chem 59: 4415–4427. [PubMed: 26565590]

Lu JY, Verkruyse LA, Hofmann SL (1996) Lipid thioesters from acylated proteins accumulate in infantile neuronal ceroid lipofuscinosis: correction of the defect in lymphoblasts by recombinant palmitoyl-protein thioesterase. Proc Natl Acad Sci U S A 93: 10046–10050. [PubMed: 8816748]

Matharu N, Rattanasopha S, Tamaru S. et al. (2019) CRISPR-mediated activation of a promoter or enhancer rescues obesity caused by haploinsufficiency. Science 363:246

McCormick PJ, Dumaresq-Doiron K, Pluviose AS et al. (2008) Palmitoylation controls recycling in lysosomal sorting and trafficking. Traffic 9: 1984–1997. [PubMed: 18817523]

Metcalf DJ, Calvi AA, Seaman MNJ et al. (2008) Loss of the Batten disease gene CLN3 prevents exit from the TGN of the mannose 6-phosphate receptor. Traffic 9: 1905–1914. [PubMed: 18817525]

Mole SE, Cotman SL (2015) Genetics of the neuronal ceroid lipofuscinoses (Batten disease). Biochim Biophys Acta 1852: 2237–2241. [PubMed: 26026925]

Mole SE, Anderson G, Band HA et al. (2019) Clinical challenges and future therapeutic approaches for neuronal ceroid lipofuscinosis. Lancet Neurol. 18:107–116. [PubMed: 30470609]

Patterson MC, Vecchio D, Prady H et al. (2007) Miglustat for treatment of Niemann-Pick C disease: a randomised controlled study. Lancet Neurol. 6: 765–772. [PubMed: 17689147]

Paushter DH, Du H, Feng T et al. (2018) The lysosomal function of progranulin, a guardian against neurodegeneration. Acta Neuropathol 136: 1–17. [PubMed: 29744576]

Perera RM, Stoykova S, Nicolay BN et al. (2015) Transcriptional control of autophagy-lysosome function drives pancreatic cancer metabolism. Nature 524:361–365. [PubMed: 26168401]

Proia RL, Wu YP (2004) Blood to brain to the rescue. J Clin Invest 113:1108–1110 [PubMed: 15085187]

Reczek D, Schwake M, Schröder J et al. (2007). LIMP-2 is a receptor for lysosomal mannose-6-phosphate-independent targeting of beta-glucocerebrosidase. Cell 131: 770–783. [PubMed: 18022370]

Santavuori P, Haltia M, Rapola J et al. (1973) Infantile type of so-called neuronal ceroid-lipofuscinosis. 1. A clinical study of 15 patients. J Neurol Sci 18: 257–267. [PubMed: 4698309]

Sarkar C, Chandra G, Peng S et al. (2013) Neuroprotection and lifespan extension in Ppt1 (−/−) mice by NtBuHA: therapeutic implications for INCL. Nat Neurosci 16: 1608–1617. [PubMed: 24056696]

Schweizer A, Kornfeld S, Rohrer J (1996) Cysteine34 of the cytoplasmic tail of the cation-dependent mannose 6-phosphate receptor is reversibly palmitoylated and required for normal trafficking and lysosomal enzyme sorting. J Cell Biol 132: 577–584. [PubMed: 8647889]

Sidransky E, Nalls MA, Aasly JO et al. (2009) Multicenter analysis of glucocerebrosidase mutations in Parkinson's disease. N Engl J Med 361: 1651–1661. [PubMed: 19846850]

Stone DL, Tayebi N, Orvisky E et al. (2000) Glucocerebrosidase gene mutations in patients with type 2 Gaucher disease. Hum Mutat 15: 181–188. [PubMed: 10649495]

Tayebi N, Parisiadou L, Berhe B et al. (2017) Glucocerebrosidase haploinsufficiency in A53T α-synuclein mice impacts disease onset and course. Mol Genet Metab 122: 198–208. [PubMed: 29173981]

Van Diggelen OP, Keulemans JL, Winchester B et al. (1999) A rapid fluorogenic palmitoyl-protein thioesterase assay: pre- and postnatal diagnosis of INCL. Mol Genet Metab 66: 240–244. [PubMed: 10191108]

Vesa J, Hellsten E, Verkruyse LA, et al. (1995) Mutations in the palmitoyl protein thioesterase gene causing infantile neuronal ceroid lipofuscinosis. Nature 376: 584–587. [PubMed: 7637805]

Wang P, Ju W, Wu D et al. (2011) A two-dimensional protein fragmentation-proteomic study of neuronal ceroid lipofuscinoses: identification and characterization of differentially expressed proteins. J Chromatogr B Analyt Technol Biomed Life Sci 879: 304–316.

Zhang Z, Lee YC, Kim SJ et al. (2006) Palmitoyl-protein thioesterase-1 deficiency mediates the activation of the unfolded protein response and neuronal apoptosis in INCL. Hum Mol Genet 15:337–346. [PubMed: 16368712]

Zhong N (2001) Molecular genetic testing for neuronal ceroid lipofuscinoses. Adv Genet 45: 141–158. [PubMed: 11332770]

Zoncu R, Bar-Peled L, Efeyan A et al. (2011) mTORC1 senses lysosomal amino acids through an inside-out mechanism that requires the vacuolar H(+)-ATPase. Science 334:678–683. [PubMed: 22053050]

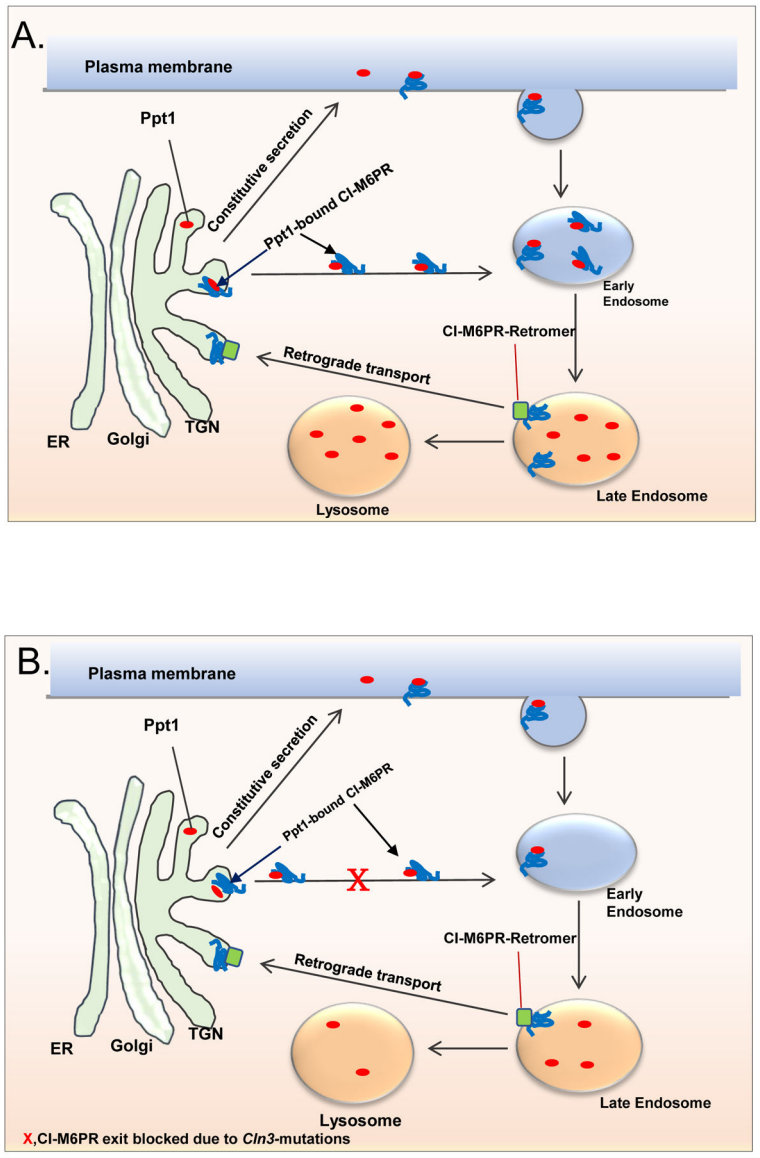

Figure 1: Schematic showing the transport of soluble proteins/enzymes from the TGN to the late endosome/lysosome by M6PR.

A.In normal cells the transport of lysosomal soluble proteins like the PPT1 from the trans Golgi network (TGN) to the late endosome/lysosome is mediated by interaction of mannosylated Ppt1 with the mannose 6-phosphate receptor (M6PR). The PPT1-M6PR complex is transported to the late endosome where the acidic pH dissociates the PPT1-receptor complex. The M6PR is then retrieved from the endosomes to the TGN by retrograde transport system that includes retromer and TIP47 and other components (see Braulke and Bonifacino, 2009). A small fraction of the cargo and the M6PR migrates to the plasma membrane and enters the endosomal pathway to the lysosome.

B. In JNCL cells in which *CLN3* is mutated, the exit of M6PR from the TGN is impaired as previously reported (see Metcalf et al 2008). We hypothesized that since CI-M6PR mediates the transport of PPT1 to the late endosome/lysosome, CLN3 mutations may lead to

lysosomal insufficiency of PPT1. **X**, Indicates blocked trafficking of M6PR-PPT1 complex from the TGN to the late endosome/lysosome.

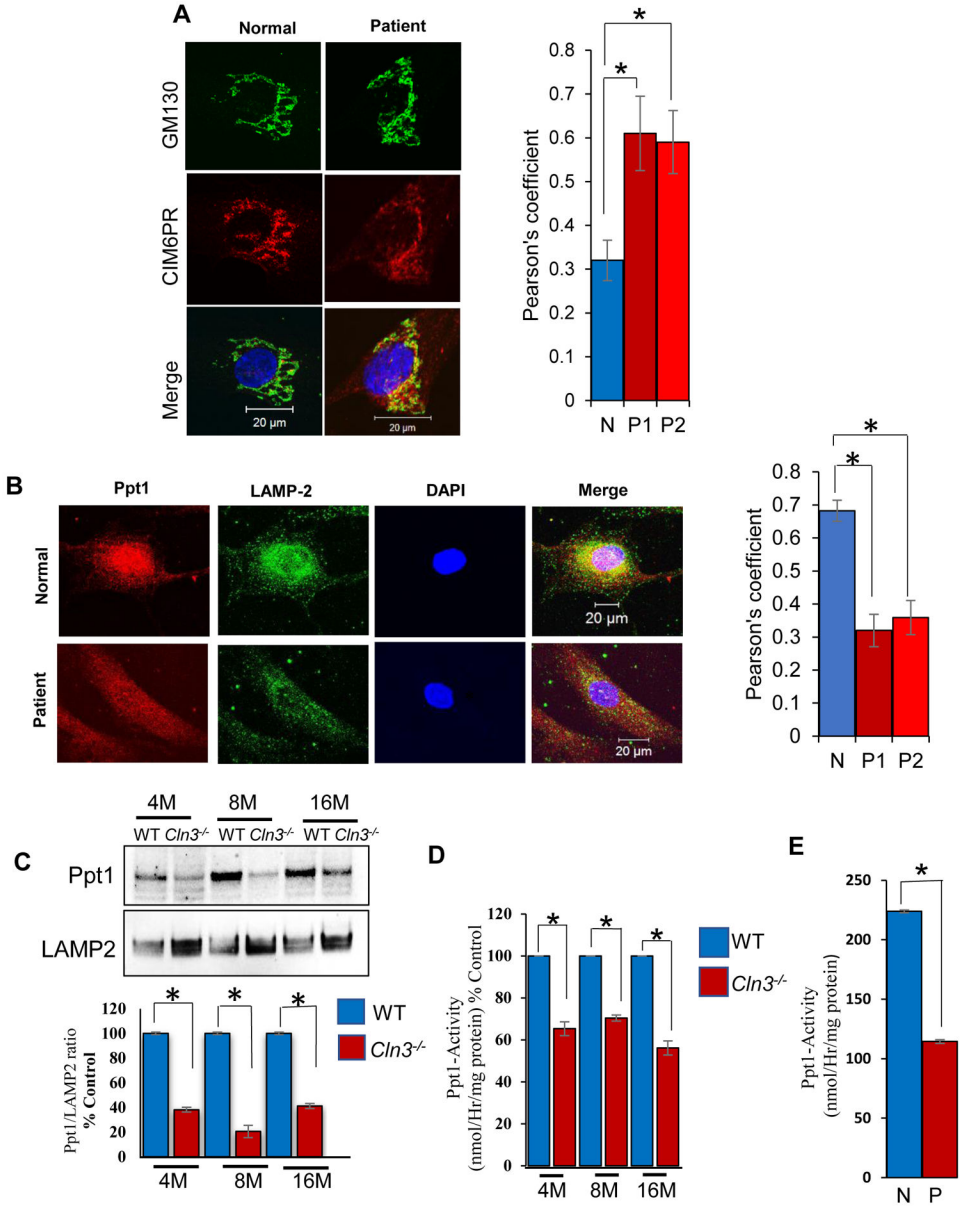

Figure 2: M6PR-mediated transport of PPT1 in normal and JNCL fibroblasts

A. Confocal imaging showing colocalization of CI-M6PR fluorescence with that of Golgi marker, GM-130 [Control (n=30), Patient#1 (n=30) and Patient#2 (n=30)] *p<0.05. Note significantly increased colocalization suggesting impaired exit of CI-M6PR from the TGN in *Cln3*$^{-/-}$ mouse brain; **B.**Confocal imaging to show significantly reduced colocalization of Ppt1 and LAMP2 (lysosomal marker) immunofluorescence in cultured cells from JNCL fibroblasts compared with normal (N) fibroblasts. [Control (n=30), Patient#1 (n=30) and Patient#2 (n=30)] *p<0.05. Both Fig. 2A and 2B lower panel are representative image of fibroblast from patient 1. **C.** Western blot analysis of Ppt1-protein levels in brain lysosomes of 4-, 8-, and 16-mont h old WT and *Cln3*-mutant mice (n=4); *p<0.05; **D.** Lysosomal Ppt1-enzyme activity in 4-, 8-, and 16-month old WT and *Cln3*-mutant mice (n=6); *p<0.05; **E.**

Ppt1 enzyme activity in cultured cells from normal (N) and JNCL patient (P). (n=3); *p<0.05.

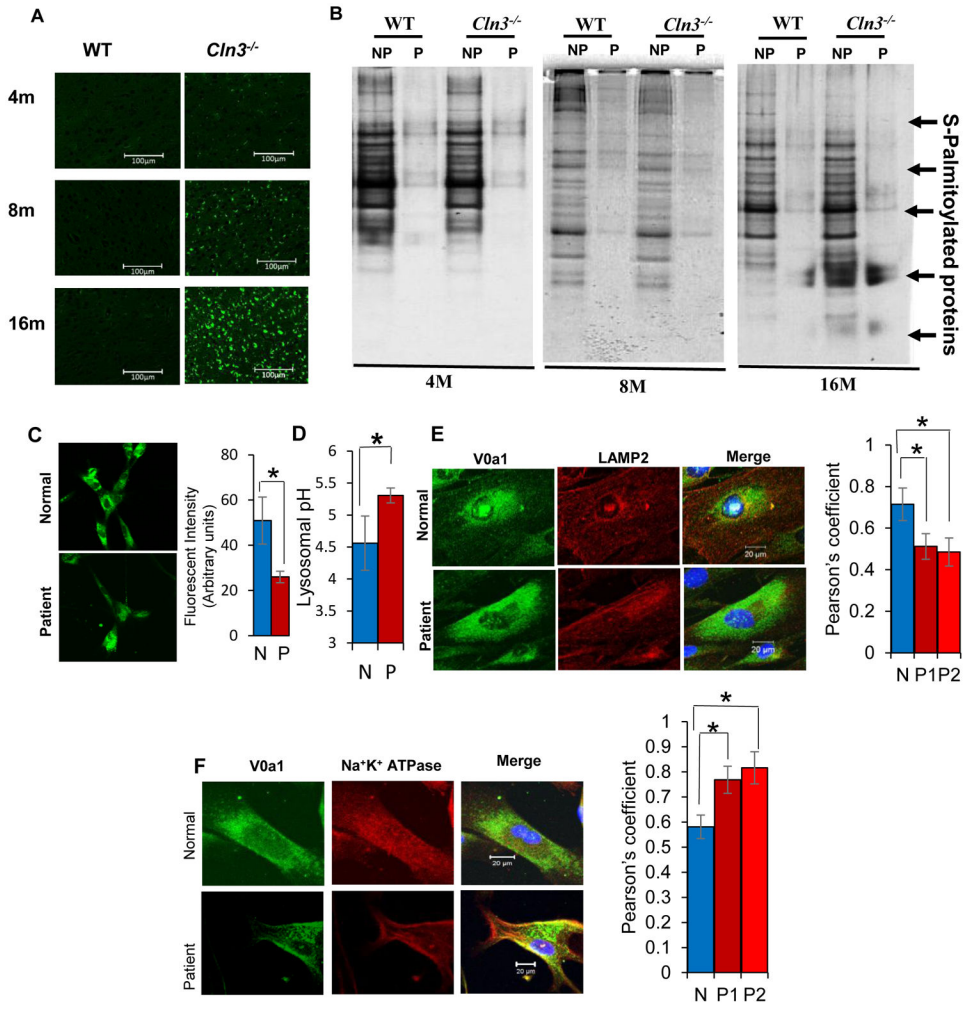

Figure 3. *CLN3*-mutations alter the levels of autofluorescence, S-acylated proteins and lysosomal pH in JNCL fibroblasts.

A. Compared to WT controls, age-dependent progressive increase of autofluorescence in the brain cortex of 4-, 8- and 16-month old *Cln3*-mutant mice. **B.** Accumulation of S-palmitoylated proteins in the lysosomes of 4-, 8- and 16-M old WT and *Cln3*-mutant mice (n=3). **C.** Qualitative determination of lysosomal pH in the normal (N) and JNCL patient (P) fibroblasts. **D.** Quantitative determination of lysosomal pH in normal and JNCL patient fibroblasts. Values expressed as the mean ± SD of three different experiments (n=3, *p<0.05). **E.** Confocal imaging showing colocalization of V0a1 fluorescence with that of lysosomal marker, LAMP2. Note significantly decreased colocalization of PPT1-signal with LAMP2 suggesting lysosomal PPT1 insufficiency in fibroblasts from JNCL patient [Control (n=30), Patient#1 (n=30) and Patient#2 (n=30)] *p<0.05. Fig. 3E lower panel is a representative image of fibroblast from patient 1. **F**. Confocal imaging showing colocalization of V0a1 fluorescence with that of membrane marker, Na^+K^+ATPase. Note significantly increased colocalization suggesting the misrouting of V0a1 to the cell membrane of JNCL patient fibroblasts compared with normal fibroblasts (N) [Control

(n=30), Patient#1 (n=30) and Patient#2 (n=30)] *p<0.05. Fig. 3F lower panel is representative image of fibroblast from patient 1.